Modulation of PD-L1 expression by standard therapy in head and neck cancer cell lines and exosomes

ANNETTE AFFOLTER[1], KAI LIEBEL[1], LUISA TENGLER[1], ELENA SEIZ[1], MORITZ TIEDTKE[1], ALEXYA AZHAKESAN[1], JULIA SCHÜTZ[1], MARIE-NICOLE THEODORAKI[2], JOHANN KERN[1], ARNE M. RUDER[3,4], JENS FLECKENSTEIN[3], CLEO-ARON WEIS[5,6], KAREN BIEBACK[7], BENEDIKT KRAMER[1], ANNE LAMMERT[1], CLAUDIA SCHERL[1], NICOLE ROTTER[1] and SONJA LUDWIG[1]

[1]Department of Otorhinolaryngology, Head and Neck Surgery, University Hospital Mannheim, Medical Faculty Mannheim of Heidelberg University, D-68167 Mannheim; [2]Department of Otorhinolaryngology, Head and Neck Surgery, University Hospital Ulm, D-89075 Ulm; [3]Department of Radiation Oncology, University Hospital Mannheim, Medical Faculty Mannheim of Heidelberg University, D-68167 Mannheim; [4]Department of Radiation Oncology, University Hospital Heidelberg, D-69120 Heidelberg; [5]Department of Pathology, University Hospital Mannheim, Medical Faculty Mannheim of Heidelberg University, Mannheim; [6]Department of Pathology, Heidelberg University Hospital; [7]Institute of Transfusion Medicine and Immunology, Medical Faculty Mannheim, Heidelberg University, German Red Cross Blood Donor Service Baden-Württemberg-Hessen, D-68167 Mannheim, Germany

Received November 25, 2022; Accepted May 15, 2023

DOI: 10.3892/ijo.2023.5550

Abstract. Although checkpoint inhibitors (CPI) have recently extended the treatment options and improved clinical response of advanced stage head and neck squamous cell carcinoma (HNSCC), treatment success remains unpredictable. Programmed cell death ligand-1 (PD-L1) is a key player in immunotherapy. Tumor cells, and exosomes derived therefrom, are carriers of PD-L1 and efficiently suppress immune responses. The aim of the present study was to analyze the influence of established therapies on PD-L1 expression of HNSCC cell lines and their exosomes. The HNSCC cell lines, UM-SCC-11B, UM-SCC-14C and UM-SCC-22C were treated with fractionated radiotherapy (RT; 5x2 Gy), cisplatin (CT) and cetuximab (Cetux) as monotherapy, or combined therapy, chemoradiotherapy (CRT; RT and CT) or radioimmunotherapy (RT and Cetux). The expression of PD-L1 and phosphorylated (p)ERK1/2 as a mediator of radioresistance were assessed using western blotting, immunohistochemistry and an *ex vivo* vital tissue culture model. Additionally, exosomes were isolated from concentrated supernatants of the (un-)treated HNSCC cell lines by size exclusion chromatography. Exosomal protein expression levels of PD-L1 were detected using western blotting and semi-quantitative levels were calculated. The functional impact of exosomes from the (un-)treated HNSCC cell lines on the proliferation (MTS assay) and apoptosis (Caspase 3/7 assay) of the untreated HNSCC cell lines were measured and compared. The HNSCC cell lines UM-SCC-11B and UM-SCC-22B showed strong expression of pERK1/2 and PD-L1, respectively. RT upregulated the PD-L1 expression in UM-SCC-11B and UM-SCC-14C and in exosomes from all three cell lines. CT alone induced PD-L1 expression in all cell lines. CRT induced the expression of PD-L1 in all HNSCC cell lines and exosomes from UM-SCC-14C and UM-SCC-22B. The data indicated a potential co-regulation of PD-L1 and activated ERK1/2, most evident in UM-SCC-14C. Exosomes from irradiated UM-SCC-14C cells protected the unirradiated cells from apoptosis by Caspase 3/7 downregulation. The present study suggested a tumor cell-mediated regulation of PD-L1 upon platinum-based CRT in HNSCC and in exosomes. A co-regulation of PD-L1 and MAPK signaling response was hypothesized.

Correspondence to: Dr Annette Affolter, Department of Otorhinolaryngology, Head and Neck Surgery, University Hospital Mannheim, Medical Faculty Mannheim of Heidelberg University, Theodor-Kutzer-Ufer 1-3, D-68167 Mannheim, Germany
E-mail: annette.affolter@umm.de

Key words: programmed death ligand-1, head and neck squamous cell carcinomas, cetuximab, MAPKs, exosomes, small extracellular vesicles

Introduction

Patients with recurrent or metastatic head and neck squamous cell carcinoma (R/M HNSCC) have few treatment options with little or no lasting response to therapy (1). With the introduction of checkpoint inhibitors (CPI), a new choice for head and neck tumors arrived. For R/M HNSCC, immunotherapy with the programmed cell death ligand-1 (PD-L1) inhibitors pembrolizumab (alone or in combination with chemotherapy) and nivolumab as a monotherapy are already established as first- and second-line therapies (2,3).

A number of tumor entities, including HNSCC, express PD-L1 and PD-L2, which interact with their programmed cell death-1 (PD-1) receptor to limit the function of activated T cells (4). There is growing knowledge about the molecular processes that induce the expression of PD-L1 and PD-L2 or modulate their protein stability (5,6). In 40% of HNSCC, there is an inflammatory phenotype with tumor-infiltrating lymphocytes. This plus the known high mutation rate resulting in the expression of possibly immunogenic neo-antigens justifies the use of CPI (7).

PD-1 antibodies are the first immunotherapeutic agents that were able to produce a stable response and a reduced mortality rate in R/M HNSCC patients (8-11). However, the number of patients who respond to CPI is low (8,11) which requires an improved prediction of therapy success. PD-L1 expression is widely used as a biomarker to predict response to CPI (12). However, especially in a heterogeneous disease such as HNSCC, a multitude of additional/other predictors are essential for diagnosis, monitoring and prediction of disease progression and therapeutic outcome (response/failure). It has been suggested that exosomes as a liquid biomarker can indicate an active HNSCC disease (13). Exosomes are nano-sized lipid vesicles ranging from 30-150 nm in size and are among the smallest of all extracellular vesicles, also called small extracellular vesicles (sEVs). Exosomes re-assemble the cargo of their parent cells reflecting the immunosuppressive molecular profiles (14-17). Tumor cells are particularly efficient exosome producers and utilize exosomes to reliably inhibit anti-tumor immune responses and thus contribute to immune evasion (13). Data indicate that PD-1 and PD-L1 expression on exosomes from HNSCC patients can be used as surrogate markers for disease progression and therapeutic response following surgery and/or chemoradiotherapy (CRT) (18-20). Data from melanoma and non-small cell lung cancer imply that exosomal PD-L1 is an early indicator for therapeutic response to anti-PD-1 CPI (21,22). However, studies on HNSCC are still rare.

At present, CPI is approved in combination with platinum-based chemotherapy or as monotherapy as it has been demonstrated that radiotherapy (RT) exerts immunomodulatory effects followed by additional immune activation (23). Currently, the effect of combinatorial treatment consisting of CPI and (C) RT in HNSCC is the subject of various clinical trials (ClinicalTrials.gov Identifier: NCT03480672, NCT03532737, NCT03349710 and numerous others). These trials note that patient sub-stratification prior to therapy selection is clearly indicated (24) and exosomal PD-L1 expression could be a valuable tool for sub-stratification.

In light of these studies, it was considered crucial to explore the effect of established therapies such as RT, platinum-based chemotherapy (CT), combined CRT and cetuximab (Cetux), an antibody against EGFR, on PD-L1 expression.

To the best of the authors' knowledge, this is the first study to address the effect of combined CT with normal-fractionated RT on checkpoint regulation, a combination that is considered standard either in the definitive or adjuvant setting for HNSCC treatment. It was hypothesized that checkpoint modulation may affect treatment response to immunotherapy in the same or subsequent therapy lines. Additionally, the present study hypothesized interrelations between PD-L1 modulation in cell lines and exosomes and signaling cascades in HNSCC known to mediate survival and therapy resistance, such as MEK/ERK.

Materials and methods

Cell culture. The cell lines UM-SCC-11B, UM-SCC-14C and UM-SCC-22B were obtained from Dr T.E. Carey (University of Michigan, Ann Arbor, MI, USA). Origins of the cell lines were larynx, oral cavity and hypopharynx, respectively (Table I) (25). Original tumors were not human papilloma virus-driven. The cells were cultivated in Dulbecco's modified Eagle's medium (DMEM; Thermo Fisher Scientific Inc.) supplemented with 10% fetal calf serum (FCS) (exosome-depleted for some experiments) and 1% penicillin/streptomycin (Gibco; Thermo Fisher Scientific, Inc.).

Reagents and antibodies. The EGFR inhibitor Cetux (Merck KGaA) was dissolved in 0.9% sodium chloride and stored in aliquots, in accord with the manufacturer's instructions. Cisplatin was dissolved in DMSO according to the manufacturer's instructions (cat. no. NSC 119875; Selleck Chemicals GmbH). Details and concentrations are summarized in the specific experiments. Appropriate concentrations of the respective compounds were determined by previous titration experiments (data not shown).

Immunohistochemistry. Cells (20,000) were seeded in 8 well chamber slides (Sarstedt, Inc.), cultured for 24 h at 37˚C and fixed by ice-cold ethanol/acetone (2:1) followed by endogenous peroxidase blockage with DAKO Peroxidase blocking solution (Agilent Technologies Deutschland GmbH). After preincubation with sheep normal serum 1:10 (BIOZOL Diagnostica Vertrieb GmbH) for 30 min at room temperature to avoid unspecific binding, primary antibodies [phosphorylated (p)44/42 MAPK (ERK1/2) (Thr202/Tyr204) cat. no. 9201, CST, Inc., 1:200; ERK1/2, cat. no. 9102, CST, Inc., 1:100; PD-L1, cat. no. 13684, CST, Inc., 1:200] were incubated overnight at 4˚C, followed by biotinylated secondary anti-rabbit or anti-mouse antibodies (Cytiva Europe GmbH, cat no. RPN 1004 and cat. no. RPN 1001) diluted 1:200 in streptavidin biotinylated horseradish peroxidase for 45 min at room temperature. Afterwards, 3-amino-9-ethylcarbazole (AEC; ScyTek Biotech Life Sciences) was added. All washing procedures were performed in PBS. Slides were counterstained by quickly dipping into hematoxylin at room temperature. Sections incubated without the primary antibody served as negative controls. Controls were also performed with the secondary antibody only (data not shown).

Irradiation experiments. Cells (20,000) from each cell line were seeded per well in six-well plates and irradiated day 2 post-seeding on five consecutive days with a daily dose of 2 Gy by the use of a linear accelerator with a photon energy of 6 MV (Synergy; Elekta AB) and polymethylmethacrylate plates as water and tissue equivalents, respectively, or kept untreated as controls. Separate lots were additionally treated with Cetux (5 μg/ml) and cisplatin (1 and 5 μM), respectively, at 37˚C on days 3, 5 and 7 in the course of change of media. Cells were left to recover again on days 8 and 9 and were

Table I. Characteristics of the HNSCC cell lines (25).

Characteristic	UM-SC-11B	UM-SCC-14C	UM-SCC-22B
Specimen	Primary	Local recurrence	Primary
Tumor site	Larynx	Floor of mouth	Hypopharynx
TNM status	T2N2a	T2N0	T2N1
Previous therapy	CT	Su+CRT	None

HNSCC, head and neck squamous cell carcinoma; Su, surgery; CT, chemotherapy; CRT, chemoradiotherapy.

harvested on day 10. Controls were mock-treated. Each experiment was performed three times.

Western blot analysis. Cells were washed with PBS and lysed with ice-cold RIPA Buffer (MilliporeSigma). The protein concentration of RIPA lysates was measured by DC Protein assay (Bio-Rad Laboratories Inc.) according to the manufacturer's instructions. A volume of homogenate containing 20 μg of total protein was separated by SDS-PAGE. Gradient gels (4-12%) were transferred to polyvinylidene fluoride membranes and blotted using primary antibodies [Phospho-p44/42 MAPK (ERK 1/2) (Thr202/Tyr204); cat. no. 9101; CST, Inc.; 1:1,000; p44/42 MAPK (ERK1/2); cat. no. 9102; CST, Inc.; 1:1,000; PD-L1; cat. no. 13684; CST, Inc.; 1:1,000; GAPDH; cat. no. 5174; CST Inc.; 1:10,000] (overnight at 4˚C, with shaking) and HRP-conjugated secondary anti-rabbit or anti-mouse antibodies (Invitrogen; Thermo Fisher Scientific, Inc.; cat. no. 31460 and cat. no. 31450; 1:10,000; 1 h at room temperature). Blocking reagents were 5% BSA (MilliporeSigma) and 5% milk (MilliporeSigma), respectively, according to the manufacturer's instructions, for 1 h at room temperature. For luminescence detection, the membrane was coated with 1 ml luminol and 1 ml peroxide solution and then analyzed with an iBright FL 1000 (Invitrogen; Thermo Fisher Scientific, Inc.). Densitometric quantification was performed using the gel analysis function of ImageJ (National Institutes of Health; Version 2.9.0/1.53t).

Ex vivo treatment of HNSCC vital tissue cultures. Fresh tissue HNSCC samples (n=9, five from the oropharynx, two from the oral cavity, two from the larynx) were procured immediately after surgical resection at the Department of Otorhinolaryngology, Head and Neck Surgery, Mannheim University Hospital, Germany. Informed written consent was obtained from all patients after the review of the local ethics board (approval no. 2019-528N). Samples were processed as previously described (26). For *ex vivo* analysis of tumor response to cisplatin, tumor sections were maintained in twelve-well plates with inserts (Thinsert; Greiner Bio One Ltd.) in DMEM, supplemented with 10% fetal bovine serum and antibiotics (penicillin 100 U/ml and streptomycin 100 μg/ml) at 37˚C. After 1 day in culture, samples were treated with cisplatin (80 mg/m^2) on days 1, 3 and 7 after change of media at 37˚C. Non-treated controls were processed in parallel. The tissue slices were harvested on day 10 to be evaluated for histopathological and immunohistochemical analysis.

Morphological and immunohistochemical evaluation of ex vivo models. *Ex vivo* cultivated tissue was formalin-fixed and paraffin-embedded (FFPE) using an automatic embedding machine. From these FFPE tissue blocks, 0.5 μm sections were cut and deparaffinized. Hematoxylin (10 min) and eosin staining (10 min) was performed at room temperature to visualize tissue morphology. Anti-Ki-67 (cat. no. M7420; Proteintech Group, Inc.; 1:50) was used to assess the proliferative activity of the tumor samples. PD-L1 expression was visualized by mAb PD-L1 (E1L3N®) XP® (cat. no. 13684; CST, Inc.; 1:200). Incubation with the primary antibodies was at 4˚C overnight. A secondary biotinylated multilink secondary anti-rabbit antibody (cat. no. RPN 1004V; Cytiva; 1:200) served for protein detection. This step was followed by the application of H_2O_2 (7%) for 7 min, then Streptavidin-Biotinylated HRP Complex (Cytiva) was added for 45 min. For staining AEC (ScyTek Biotech Life Sciences) was used. Precipitate development of the substrate solution was monitored under the microscope. The sections were counterstained with hematoxylin by quickly dipping at room temperature. For PD-L1 expression, the TPS (tumor proportion score) was evaluated by two independent observers. The number of positively membrane-bound stained tumor cells was divided by the number of all tumor cells.

Exosome isolation from cell supernatants. For exosome enrichment, HNSCC cell lines were cultured in two to three T75 culture flasks, treated and irradiated according to the aforementioned protocol and the medium was collected on days 5, 7 and 10. Medium with exosome-depleted FCS was used for this experiment: Bovine exosomes were removed from the serum by centrifugation at 120,000 x g and 4˚C for 18 h.

Exosomes from cell culture supernatants were prepared by size exclusion chromatography as previously described by Hong *et al* (27): Briefly, conditioned cell culture medium was differentially centrifuged at 2,000 x g for 10 min at room temperature and at 14.000 x g for 30 min at 4˚C, followed by ultrafiltration (Millipore filter, 0.22 μm). The medium was concentrated 50 x using Vivaspin® 20 concentrators with an molecular weight cutoff of 100,000 Da (Sartorius AG; cat. no. VS2041). Self-made mini size exclusion chromatography columns were prepared. The fourth fraction, verified to contain exosomes, was collected and used for further studies.

Nanoparticle tracking analysis (NTA). NTA was performed on ZetaView (Particle Metrix GmbH) to determine the size distribution and concentration of the isolated particles. Freshly prepared exosome samples were diluted at 1:50-1:1,000 in PBS and measured at 11 test ranges with two cycles. Concentration and size ranges were calculated by NTA 2.0 analytical software (Particle Metrix GmbH).

Transmission electron microscopy (TEM) of exosomes. TEM was conducted as previously described at the Electron Microscopy Core Facility of Heidelberg University (20). Freshly prepared exosomes were placed on carbon-coated formvar grids with 3% w/v uranyl acetate at room temperature for ~3 sec. Exosomes were visualized by a JEM1400

transmission electron microscope (JEOL Ltd.) with a bottom-mounted 4K CMOS camera (TemCam F416; TVIPS). Micrographs were analyzed using ImageJ (National Institutes of Health; Version 2.9.0/1.53t).

Measurement of protein content. The protein content of the isolated exosomes was analyzed using Pierce BCA protein assay (Thermo Fisher Scientific, Inc.) according to the manufacturer's instructions.

Western blotting of exosomes. Exosomes (10 μg) were lysed in reducing sample buffer (Thermo Fisher Scientific, Inc.; cat. no. 39000). Samples were loaded onto 4-20% precast gels (Bio-Rad Laboratories, Inc.; cat. no. 4561094) and SDS-PAGE was performed, followed by protein transfer onto a PVDF membrane. The membrane was blocked using 5% skimmed milk in TBST (0.1% Tween-20) for 1 h at room temperature and incubated with primary antibodies overnight under refrigeration (TSG101; cat. no. PA5-31260; Invitrogen; Thermo Fisher Scientific, Inc.; 1:500; CD63; cat. no. 10628D; Invitrogen; Thermo Fisher Scientific, Inc.; 1:250; CD9; cat. no. 10626D; Invitrogen; Thermo Fisher Scientific, Inc.; 1:500; Grp94; cat. no. 2104; CST; 1:1,000; ApoA1; cat. no. 3350; CST; 1:1,000; TRAIL; cat. no. ab2056; Abcam; 1:500; PD-L1; cat. no. 13684; CST; 1:1,000). The membrane was exposed to the HRP-conjugated secondary anti-rabbit or anti-mouse antibody (Invitrogen, cat. no. 31460 and cat. no. 31450, 1:10,000) for 1 h at room temperature. After additional three washes, the chemiluminescent substrate (Thermo Fisher Scientific, Inc.; cat. no. 34076) was added and subsequently the membrane was imaged using an iBright FL 1000 (Invitrogen; Thermo Fisher Scientific, Inc.). Densitometric quantification was performed using the gel analysis function of ImageJ (National Institutes of Health; Version 2.9.0/1.53t).

Caspase-Glo® 3/7 assay. HNSCC cell lines were seeded in white-walled 96-well-plates at a density of 5,000 cells/well in 50 μl. The cells were immediately treated with 50 μl exosomes (1 μg) in PBS and after 24 h an equal volume of luminogenic caspase-3/7 substrate (Promega Corporation) was added and incubated at room temperature for 1 h. Luminescence was read with a Tecan Infinite® 200 PRO microplate reader (Tecan Group, Ltd.). As negative control, cells were treated with PBS.

MTS proliferation assay. HNSCC cell lines were seeded in 96-well-plates and treated with 1 μg exosomes, as described above. After 24 h the MTS reagent (Abcam) was added 1:10, incubated 3 h at 37˚C and the absorbance was measured at 490 nm. As negative control, cells were treated with PBS. In other studies, it has been shown that a reliable proliferation can be detected by the MTS assay after 24 h co-incubation (28-30).

Statistical analysis. Results were graphed and analyzed by the use of GraphPad Prism software (version 9.4.1; Dotmatics). Data were presented as means (bars) with standard error means (whiskers) of three independent experiments. For western blotting results from tumor cell lines Kruskal-Wallis tests (non-parametric, without P-value correction) were performed. Uncorrected Dunn's test was used as a post-hoc test. $P<0.05$ was considered to indicate a statistically significant difference.

Results

Heterogenic basal expression of target proteins in immunohistochemistry of the HNSCC cell lines. Basal expression levels of pERK1/2, panERK1/2 and PD-L1 were immunohistochemically assessed to illustrate the heterogeneity of the *in vitro* cell culture model. Differential expression of the markers was found in all three cell lines. Expression levels of pERK1/2 were strongest in UM-SCC-11B and weaker in UM-SCC-14C and UM-SCC22B. PD-L1 and panERK1/2 expression levels were stronger in UM-SCC-22B than in UM-SCC-11B and UM-SCC-14C (Fig. 1).

Basal and postradiogenic ERK1/2 phosphorylation is suppressed by EGFR blockade. Previously, the authors reported post-radiogenic activation of the MAPK pathway in HNSCC by a single dose irradiation (26). The present study aimed for a fractionated RT scheme adapted to the normofractionation with 5x2 Gy per week comparable to the conditions applied to HNSCC patients in the clinic (with a break at the weekend), combined with Cetux. Cetux/EGFR blockade similarly suppressed basal pERK1/2 expression most clearly in UM-SCC-14C cells. The effect was less pronounced in UM-SCC-11B and UM-SCC-22B cells. However, EGFR blockade failed to inhibit postradiogenic ERK1/2 activation in all three cell lines although EGFR is a direct upstream activator of the Ras-RAF-MEK-ERK pathway (Fig. 2; pERK1/2/tERK1/2 ratios are given in Table SIII).

Association of PD-L1 expression with ERK1/2 phosphorylation post-treatment. PD-L1 expression revealed a similar pattern in UM-SCC-14C cells with basal and postradiogenic inhibition of PD-L1 expression by EGFR blockade while UM-SCC-22B and UM-SCC-11B cell lines did not display a strong response to treatment (Fig. 2; Table SI). An association of PD-L1 checkpoint regulation and MAPK signaling which are probably co-regulated upon treatment, at least in UM-SCC-14C cells, was hypothesized.

ERK1/2 is activated by RT and cisplatin. Following combined treatment with RT and cisplatin on days 3, 5 and 7 at two different concentrations (1 and 5 μM), ERK1/2 activation was assessed. A distinct upregulation after combined RT and the high-dose cisplatin (5 μM) concentration was observed in all three cell lines indicating a potential mechanism of cellular resistance as an undesired treatment effect (Fig. 3; Table SII; Table SIV). If ERK1/2 is activated upon cancer treatment, a mechanism of cellular resistance is most likely which has been previously described (31-35). Postradiogenic cellular responses could be specified by administering inhibitors of the MAPK ERK pathway (33-35).

Cisplatin and irradiation-induced upregulation of PD-L1. After application of standard mainstays irradiation and cisplatin, all three cell lines showed a distinct and dose-dependent increase of PD-L1 expression levels after cisplatin alone.

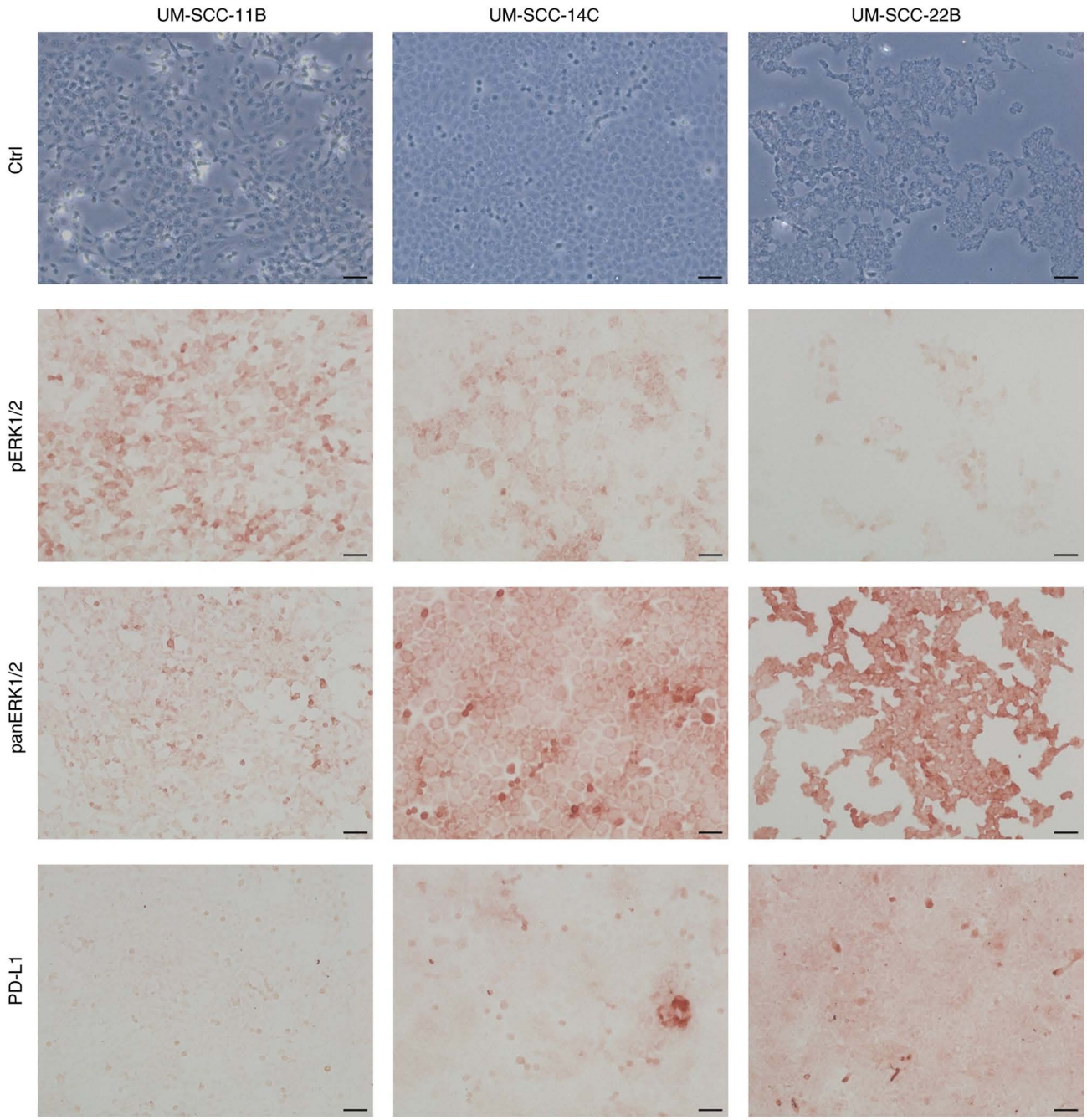

Figure 1. Immunohistochemical staining for basal expression of target proteins. All cell lines were examined by immunohistochemistry for basal expression of the target proteins and, as expected, showed heterogeneous expression with different expression levels of pERK1/2, panERK1/2 as well as PD-L1, as shown. UM-SCC-11 showed the strongest expression levels of pERK1/2 while PD-L1 and panERK1/2 were expressed most markedly in UM-SCC-22B. Magnification: x200, scale bar, 50 μm. p, phosphorylated; PD-L1, programmed cell death ligand-1.

UM-SCC-14C cells displayed the strongest rise. This modulation of PD-L1 was enhanced after combined CRT. Again, the effect was most marked in UM-SCC-14C cells. Effects of single RT were negligible. Additionally, a nearly identical expression pattern for was observed all treatment combinations in these lines UM-SCC-11B and UM-SCC-14C when comparing PD-L1 with pERK1/2 levels. Taken together, these findings indicated that cisplatin acts synergistically with irradiation treatment to modulate the PD-1/PD-L1 axis. As after RT/Cetux application, PD-L1 appeared co-regulated with pERK1/2, again in UM-SCC-14C but additionally in UM-SCC-11B cell lines. Notably, the effect of combined CRT was supra-additive in these two cell lines while in 22B it was not (Fig. 3; Table SII).

Cisplatin-induced PD-L1 modulation is validated ex vivo. To refine these results and to adapt to a clinical setting, the present study investigated the effect of cisplatin (80 μM) on PD-L1 regulation in eight independent *ex vivo* tumor cultures; two samples displayed an elevated PD-L1 expression following treatment compared with controls. The other samples showed basal PD-L1 expression and cisplatin caused no induction, reflecting the distinct heterogeneity in HNSCC (Fig. 4).

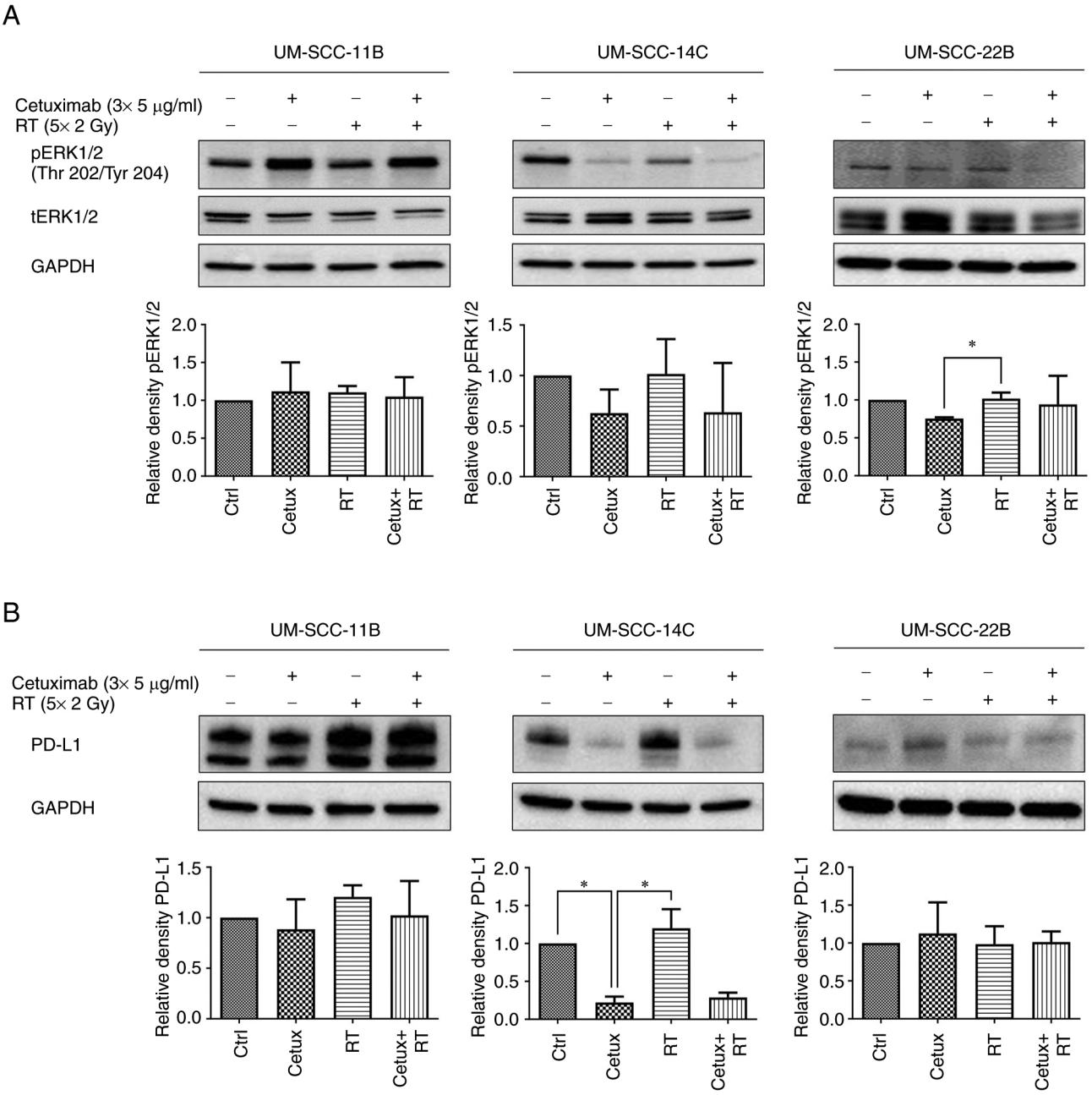

Figure 2. Impact of fractionated irradiation and Cetux on expression levels of pERK1/2, tERK1/2 and PD-L1 in UM-SCC-11B, UM-SCC-14C and UM-SCC-22B cells. Cells were irradiated in the linear accelerator by applying a fractionated scheme with 5x2 Gy on days 3-7 after seeding and/or treated with Cetux (5 μg/ml) on days 3, 5 and 7. Mock-treated cells served as control. Cells were harvested on day 10. Western blots of pERK1/2 and tERK1/2 (upper panel) and PD-L1 (lower panel) are shown. GAPDH was used as a loading control. UM-SCC-14C cells showed an association of pERK1/2 and PD-L1 expression levels with distinct basal and postradiogenic inhibition by Cetux. EGFR inhibited pERK1/2 expression in-22B cells to a lesser extent, however, MEK/ERK signaling by blockade of the upstream EGF receptor was not consequently impeded in all three cell lines. Cetux, cetuximab; p, phosphorylated; t, total; PD-L1, programmed cell death ligand-1. *P<0.05.

Characterization of exosomes. To validate the biomarker potential and the functional role of exosomes in HNSCC cell lines treated with irradiation and/or chemo- or targeted therapy, exosomes were isolated from all three cell lines and their molecular cargo and functional impact on untreated HNSCC cell lines analyzed.

The representative TEM images show typical size ranges from 30-120 nm and typical vesicular shapes of the isolated exosomes from all three cell lines (Fig. 5A). Western blots of exosomes confirm the expression of the endosomal protein (TSG101), tetraspanins (CD63 and CD9) and low expression/lack of isolation byproducts (Grp94, ApoA1) as suggested by MISEV 2018 (Fig. 5B) (36). Nanoparticle tracking analysis reveals comparable concentrations and median size ranges of the particles in the preparations from all cell lines (Fig. 5C).

Expression levels of exosomal PD-L1 and TRAIL. To assess the role of exosomes in inducing apoptosis, the apoptosis markers PD-L1 and TRAIL were detected and their relative density was compared with TSG101 in western blots for the different treatment conditions (Fig. 6; Fig. SI).

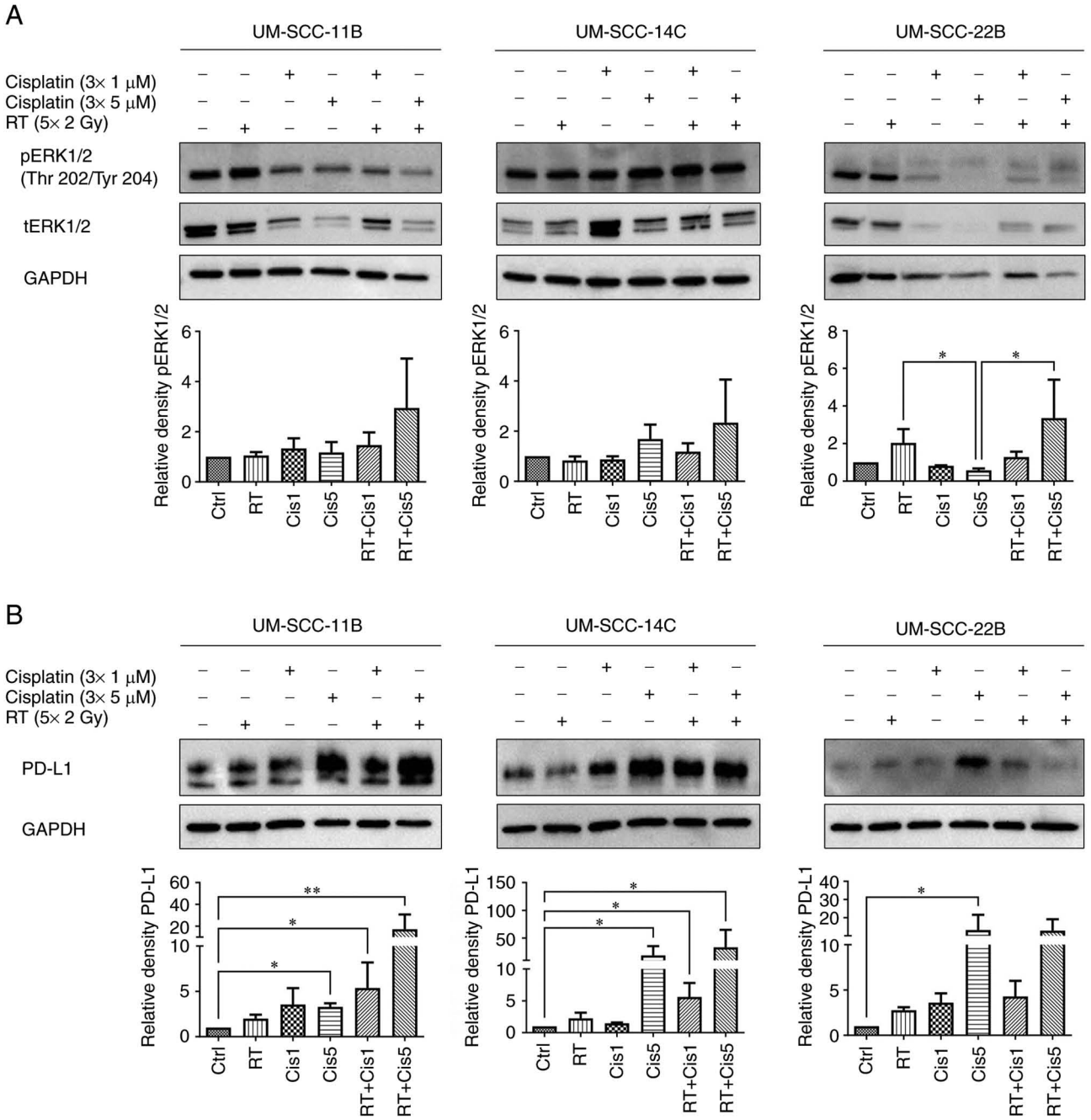

Figure 3. Impact of fractionated irradiation and cisplatin on expression levels of pERK1/2, tERK1/2 and PD-L1. Cells were irradiated in the linear accelerator by applying a fractionated scheme with 5x2 Gy on days 3-7 after seeding and/or treated with cisplatin with either 1 μM or 5 μM on days 3, 5 and 7. Mock-treated cells served as control. Cells were harvested on day 10. Western blots of pERK1/2 and tERK1/2 (upper panel) and PD-L1 (lower panel) are shown. GAPDH was used as a loading control. All three cell lines showed a strong activation of ERK1/2 by the higher concentration of cisplatin teamed with fractionated RT as well as a strong induction of PD-L1 after cisplatin treatment which was supra-additive when combined with irradiation. p, phosphorylated; t, total; PD-L1, programmed cell death ligand-1. *P<0.05; **P<0.01.

Relative PD-L1 and TRAIL expression in exosomes was induced by monotherapy with RT in all three cell lines. Notably, treatment with low-dose cisplatin (Cis1, 1 μM) resulted in higher relative PD-L1 and TRAIL expression levels in exosomes from UM-SCC-11B and UM-SCC-14C than in exosomes from UM-SCC-22B with no expression.

Markedly, exosomes from HNSCC cell lines treated with combined CRT (Cis1+RT) revealed controversial results: While PD-L1 and TRAIL showed low expression levels in exosomes from UM-SCC-11B, elevated expression levels were present in exosomes from UM-SCC-14C and UM-SCC-22B cell lines.

Exosomes from HNSCC cell lines modulate the proliferation and apoptosis of HNSCC cell lines. Exosomes from HNSCC cell lines treated with the various therapeutic conditions were co-incubated with the untreated HNSCC cell lines for 24 h to monitor the proliferation (Fig. 7A) and apoptosis (Fig. 7B). Untreated HNSCC cell lines that were co-incubated with exosomes from UM-SCC-11B post chemoradiotherapy

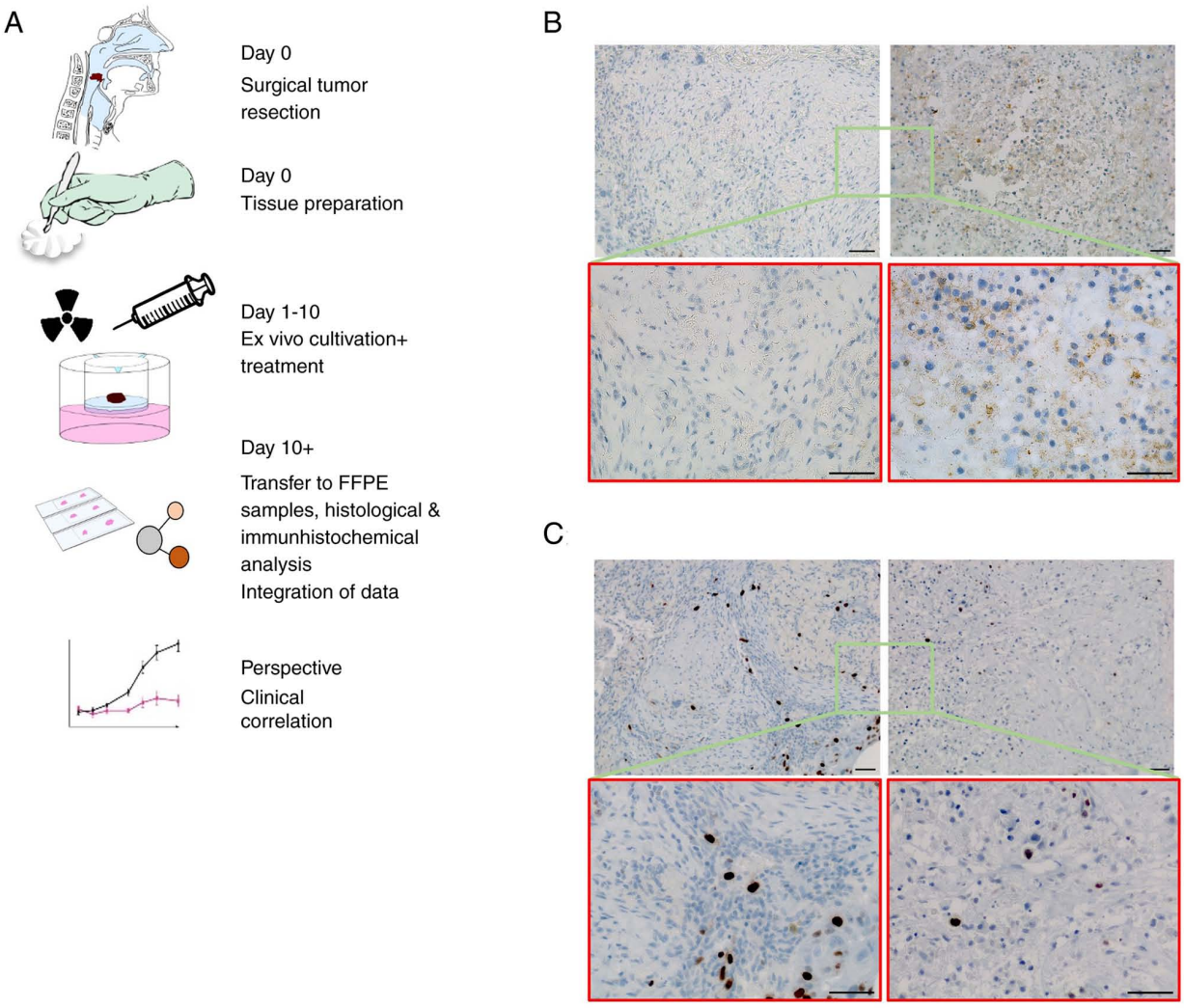

Figure 4. Immunohistochemical staining of ex vivo HNSCC tissue cultures. (A) Workflow of the experimental setting. After surgical resection, vital tumor tissues were cut into 2-3-mm-thick slides and kept in culture for up to 10 days. After experimental treatment samples were formalin-fixed and paraffin-embedded. Tissue sections were analyzed by hematoxylin and eosin staining and immunohistochemical staining. The correlation of experimental data with clinical outcome most likely offers the perspective of personalized therapy approaches. (B) Representative immunohistochemistry staining of PD-L1 in *ex vivo* tumor tissues with or without cisplatin treatment (3x80 μM). Left panel: Moderate immunostaining of PD-L1 in an untreated oropharyngeal SCC sample, scored with a TPS of 5%. Right panel: Distinct induction of PD-L1 after cisplatin treatment in corresponding samples from the same tumor, scored with a TPS of 25%. (C) Left panel: Low basal expression levels of the proliferation marker Ki-67 in untreated controls of the same OPSCC. Right panel: Further reduction of Ki-67 positive cells after cisplatin treatment. Scale bar, 50 μm. Parts of the figure were drawn by using pictures from Servier Medical Art (http://smart.servier.com/), licensed under a Creative Commons Attribution 3.0 Unported License (https://creativecommons.org/licenses/by/3.0/). HNSCC, head and neck squamous cell carcinoma; PD-L1, programmed cell death ligand-1; SCC, squamous cell carcinoma; TPS, tumor proportion score; OPSCC, oropharyngeal squamous cell carcinoma.

(Cis1+RT) revealed reduced proliferation. Exosomes from other cell lines or treatment conditions did not modulate the proliferation of the cell lines.

Exosomes from HNSCC cells treated with RT, cisplatin and CRT induced apoptosis of UM-SCC-11B and UM-SCC-22B. Strikingly, apoptosis was reduced in UM-SCC-14C co-incubated with exosomes from the irradiated (RT) cell line ($P<0.05$) and combined therapy (Cis1+RT or Cetux+RT), whereas monotherapy with chemotherapy or targeted therapy alone did not modulate apoptosis.

Discussion

Although the PD-L1 expression status is well-accepted for the medical justification of anti-PD-1 agents, the clinical success is not as high as expected and requires improved stratification. The expression of PD-L1 is undergoing changes during the clinical course and treatment reflected by altered expression levels after chemotherapeutic drugs or RT or as a response to exogenous signals (IF-y) (37). Although CRT is considered a standard therapy in HNSCC, there is only limited knowledge about direct tumor cell-dependent upregulation of PD-L1 expression upon exposure.

As taken into account in the present study and in other studies, irradiation is known to exert immunomodulatory effects and appears to activate immune responses by inducing DNA damage and cell death as inflammatory signals occur through the activation of cell survival pathways (38). Dovedi *et al* (39) postulate that acquired resistance to radiotherapy can be overcome by concomitant

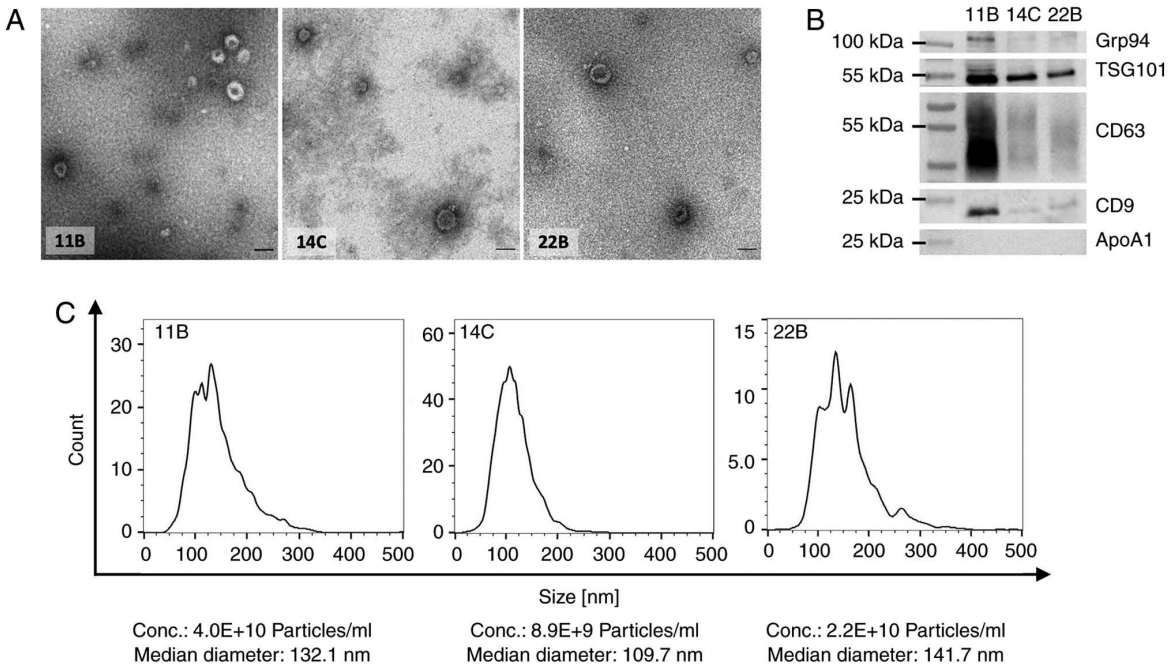

Figure 5. Morphology, size distribution, concentration and protein profiles of exosomes from HNSCC cell lines. Supernatants from HNSCC cell lines were collected and exosomes were isolated on mini-size exclusion chromatography columns. (A) Exosomes from UM-SCC-11B (11B), UM-SCC-14C (14C) and UM-SCC-22B (22B) show the typical vesicular shape and size in TEM images. Scale bar, 100 nm. (B) Western blotting was performed after loading 10 μg exosome preparation per lane and show the exosome markers TSG101, CD63 and CD9 and ApoA1 and Grp94 were used as purity control. (C) Nanoparticle tracking analysis was performed to detect median sizes and particle concentrations of the isolated particles. Representative pictures are shown of representative exosome preparations. HNSCC, head and neck squamous cell carcinoma.

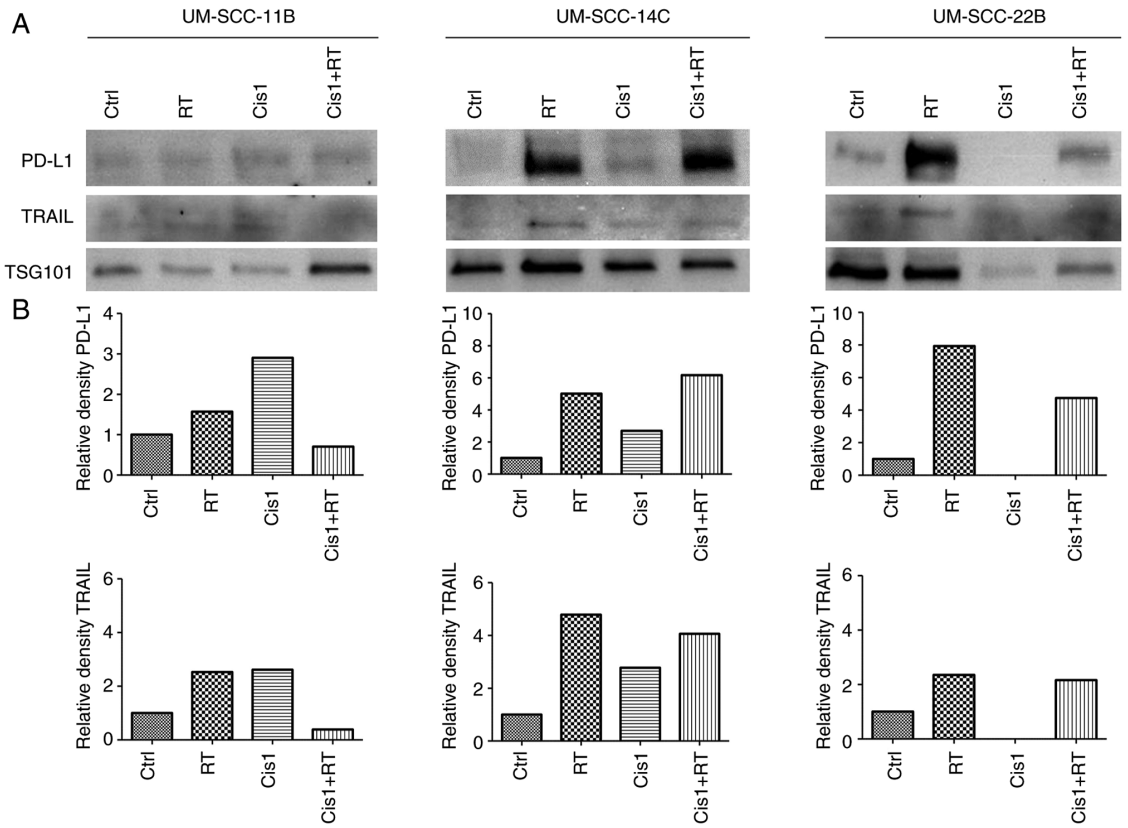

Figure 6. Protein profiles of exosomes from (un)treated HNSCC cell lines UM-SCC-11B, UM-SCC-14C and UM-SCC-22B. The HNSCC cell lines were treated with 5x2 Gy radiotherapy (RT), 1 μM cisplatin (Cis1) and as combination therapy (Cis1+RT). As a control (Ctrl), untreated cell lines were used. (A) Western blotting of exosomes from HNSCC cell lines were performed using 10 mg exosome preparation per lane. Expression levels of PD-L1, TRAIL and TSG101 were detected for the different treatment conditions and compared. (B) Semi-quantitative densitometry of western blot bands of PD-L1 and TRAIL were related as mean integrated pixel values (image intensity band area) were related to TSG101 and compared for the different therapeutic conditions. HNSCC, head and neck squamous cell carcinoma; PD-L1, programmed cell death ligand-1.

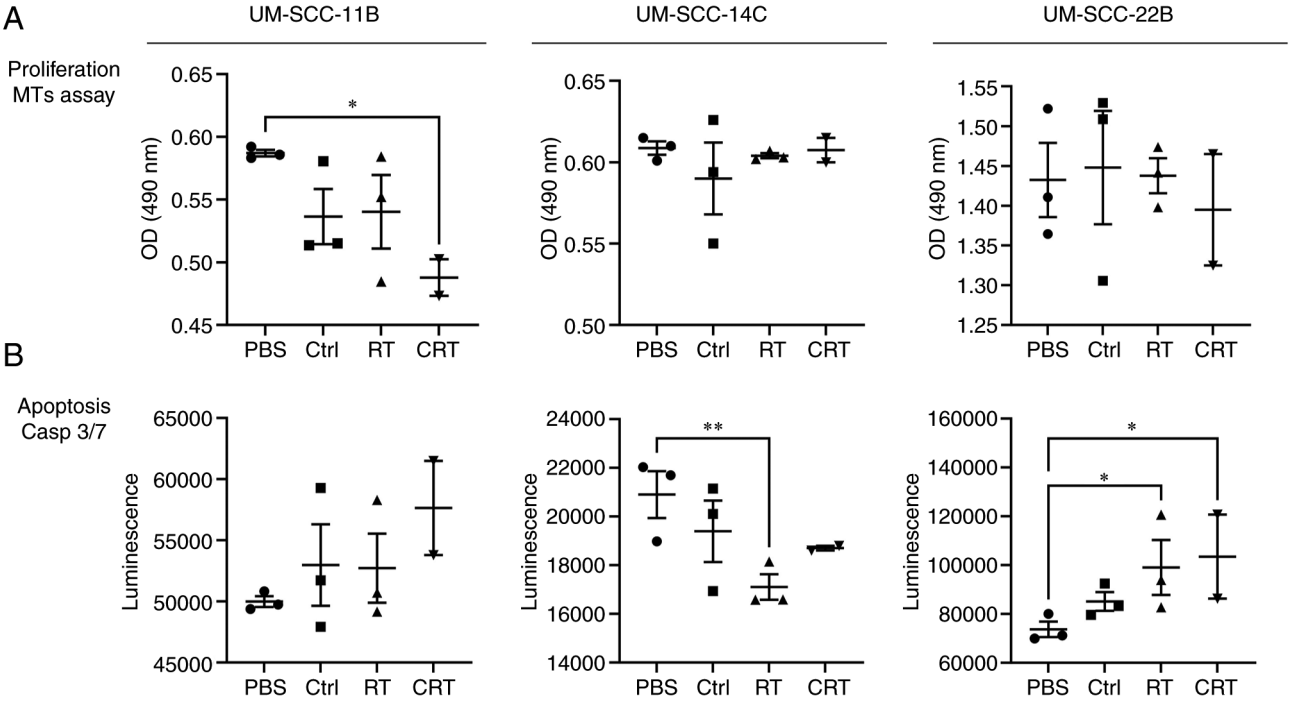

Figure 7. Proliferation and apoptosis of untreated HNSCC cell lines by exosomes from HNSCC following different treatment conditions. Exosomes were isolated from (un)treated HNSCC cell lines and co-incubated with matching untreated HNSCC cell lines for 24 h. The treatment conditions were the following: 5x2 Gy RT alone and CRT (Cis1+RT). (A) The proliferation of the HNSCC cell lines was detected using an MTS assay displaying a significant reduction of proliferation by exosomes from UM-SCC-11B treated with CRT. (B) Apoptosis was indirectly measured using the Caspase 3/7 assay. Exosomes from the irradiated HNSCC cell lines UM-SCC-11B and UM-SCC-22B induced apoptosis in the untreated HNSCC cell lines, while the exosomes from the irradiated UM-SCC-14C reduced the apoptosis. The graphs show means (bars) with standard error means (whiskers) of three independent experiments. *P<0.05; **P<0.01. HNSCC, head and neck squamous cell carcinoma; RT, radiotherapy; Cis1, cisplatin; CRT, chemoradiotherapy.

but not sequential administration of anti-PD-L1 mAb with fractionated irradiation.

Therefore it is mandatory to gain new insights into the regulation of the PD-1/PD-L1 axis upon exposure to standard head and neck cancer therapy, in particular fractionated RT combined with cytotoxic agents. As the response rate in HNSCC towards CPI is still low with <20% (40), the present study investigated the impact of fractionated RT with platinum-based chemotherapy and Cetux on PD-L1 expression in an *in vitro* HNSCC model including established tumor cell lines and their exosomes and primary patient explants.

A total of three HNSCC cell lines were used as an *in vitro* model to mimic heterogeneity in HNSCC and to improved understand patient-specific response patterns. For validation, primary tumor material derived from HNSCC patients was analyzed.

Supporting the hypothesis, a moderate increase of PD-L1 was noticed in all three cell lines and their exosomes when treated with RT alone.

Other groups have likewise observed an upregulation of PD-L1 following RT in HNSCC and other entities (41-45). For HNSCC, it has been described that an increase in PD-L1 expression in radioresistant cell lines after RT affects cell proliferation due to the inactivation of GSK-3β (46). The observed induction of PD-L1 in the HNSCC cell lines and their exosomes underlines the biomarker potential of exosomes. Lately, it was reported that PD-L1^{+} exosomes are a reliable biomarker for an active HNSCC disease and effectively inhibit CD8^{+} -T cell activity, which can be attenuated by anti-PD-1 therapy (18).

The present study discovered that exosomes from irradiated HNSCC cells reduced apoptosis in untreated UM-SCC-14C cells. Notably, Mutschelknaus *et al* (47) made similar observations; that exosomes from irradiated HNSCC cell lines promote prolonged survival of untreated HNSCC cell lines by the increase of DNA double-stranded repair. Thus, exosomes from irradiated HNSCC cell lines could be utilized as a survival mechanism by the tumor protecting the non-irradiated cells from apoptosis and thus supporting immune evasion.

The expression of PD-L1 on tumor cells, the presence of tumor-infiltrating lymphocytes and high mutational burden (48-50) indicate sensitivity towards CPI. RT inducing these features is thus very likely to increase the response. First, the observation that fractionated RT alone induces PD-L1 is a well-known and undesired side-effect causing immunosuppression (51). Oweida *et al* (52) investigated whether local irradiation can change the immunogenicity of the tumor by sensitizing a poorly immunogenic HNSCC towards PD-L1 inhibition. They observed treatment resulting in a highly inflamed tumoral phenotype and proposed an enhanced tumor cell killing by increased T cell infiltration. Likewise, Deng *et al* (53) proposed a cytotoxic T cell-dependent mechanism after combined RT and PD-L1 blockade that boosted the irradiation efficacy.

In addition, the killing of cancer and stroma cells by antigen-specific cytotoxic T lymphocytes is strengthened if the tumor antigen (Ag) is released by the application of local RT or chemotherapeutic agents Such findings indicate that

there is a rationale for developing combination treatments of irradiation or chemotherapy with CPI. (54).

Similarly, when treating with cisplatin the present study observed a distinct induction of PD-L1 expression in all three cell lines with the greatest increase in UM-SCC-14C and UM-SCC-22B cells and in exosomes from UM-SCC-11B and UM-SCC-14C, however, not from UM-SCC-22B.

In UM-SCC-14C and UM-SCC-11B, this induction was even enhanced by combining cisplatin with fractionated RT, while in exosomes an elevated induction in UM-SCC-14C and UM-SCC-22B was observed. The data of the present study are in line with previous publications: An upregulation of PD-L1 expression in HNSCC has been observed after a number of cytotoxic treatments including cisplatin, carboplatin, docetaxel, platinum and fluorouracil as summarized by Lin *et al* (55). As a mechanism, the tumor immune escape is likely to be promoted by an increase in PD-1/PD-L1 expression through the MAPK/ERK kinase pathways in HNSCC patients (37).

While these results refer to a single treatment with irradiation and cytotoxic agents, for the first time, to the best of the authors' knowledge, the present study presented an induction of PD-L1 surface expression in HNSCC upon cisplatin teamed with fractionated RT (5x2 Gy) with supra-additive effects in two cell lines compared with the application of monotherapy with cisplatin or irradiation. So far, the combined and synergistic effect of CRT on PD-L1 expression has not been described for HNSCC but has been shown in other entities backing the observations the present study (51). In melanoma, IL-6 acts as a possible further intrinsic tumor cell trigger for regulating the expression of PD-L1 after RT and CRT. Furthermore, PD-L1 upregulation occurs especially on vital tumor cells dependent on the entity (51), which could be an explanation for the heterogeneous expression depending on the location of the tumor of origin.

In any case, these data clearly indicated that standard therapy such as CRT is capable of affecting checkpoint regulation in HNSCC. The role of PD-L1 as a prognosticator has been recently addressed by various research groups for different tumor entities. PD-L1 appears to be a negative prognostic factor in NSCLC, yet remains controversially discussed (56). For HNSCC, a study indicates that tumors with high PD-L1 expression potentially follow an unfavorable clinical course (57), which is in line with other studies (58,59). In summary, patients whose tumors strongly express PD-L1 might benefit from the (early) application of CPI and it is likely to be advantageous to combine anti-PD (L)-1 agents with standard pillars.

The effect of exosomal PD-L1 as an indicator for therapeutic response has been controversially discussed in the literature: In the follow-up of HNSCC therapy after surgery and/or (C)RT high exosomal PD-L1 has been either linked to therapeutic response and improved disease-free survival (19) or active disease and worse overall survival (20). In metastatic melanoma treated with anti-PD-1 CPI, an increase of the exosomal load of PD-L1 was either correlated with therapeutic response (60) or indicated a persistent disease (61). It has been hypothesized that high exosomal PD-L1 levels following therapy are caused by immunomodulatory tumor responses hinting towards therapeutic response (62). However, another study emphasizes that the exosomal PD-L1 reflects PD-L1 expression in tumor cells and thus the tumor burden (61). These controversies underline the urgent need for larger biomarker studies since the observed obstacles might be due to different immune escape mechanisms at various time points.

By combining the EGFR blockade Cetux with fractionated RT the present study found a suppression of basal and postradiogenic pERK1/2 expression in UM-SCC-14C and, less pronounced, in UM-SCC-11B cells. However, the blockade of the EGFR failed to inhibit the Ras-RAF-MEK-ERK pathway directly downstream in all three cell lines. Notably, this basal and postradiogenic decrease after combined Cetux and RT in UM-SCC-14C cells could be similarly observed for PD-L1 expression indicating that MAPK ERK signaling and checkpoint regulation are associated in some but not all HNSCC. In exosomes, however, a slight increase in PD-L1 and almost no change in TRAIL expression was observed (Fig. S1). The functional assays revealed a decreased apoptosis in untreated UM-SCC-11B and UM-SCC-14C cells after treatment with exosomes from Cetux and irradiated cells (Fig. 7). The results of the present study may be limited by the fact that it did not measure apoptosis directly but in an indirect way by Caspase 3/7 activity.

Theodoraki *et al* (63) observed that HNSCC patients, enrolled in a phase I trial receiving a treatment combination of irradiation, Cetux and imiplimab, increased exosomal PD-L1 expression during follow-up when the disease recurred. In conclusion, the functional impact of exosomes secreted by irradiated tumor cells that protect unirradiated HNSCC cells from apoptosis might serve as one mechanism of tumor resistance and the exosomal PD-L1 expression might reflect the failed therapeutic response in HNSCC.

Notably, in contrast to Ock *et al* (37), in the present model cisplatin alone did not or only moderately increase pERK1/2, although the pERK1/2/total-ERK1/2 ratio was not determined, while Ock *et al* (37) describe an enhanced dose-dependent ratio of p-MEK/total-MEK following cisplatin treatment in HNSCC cells. Ock *et al* (37) state that MEK regulation is a crucial step in modulating PD-L1 expression in cancer. If tumor cells are resistant to anti-EGFR treatment the MEK pathway is activated and inhibition of the MEK pathway attenuates PD-L1 upregulation. An association between PD-L1 regulation and EGFR downstream signaling, especially in the case of EGFR mutations, has also been described for NSCLC (64,65). The present study discovered a potential co-regulation of PD-L1 and activated ERK1/2, most evident in UM-SCC-14C. This is in line with Ota *et al* (64), who found both EML4-ALK and mutant EGFR upregulating PD-L1 by activating PI3K-AKT and MEK-ERK signaling pathways in NSCLC which reveals a direct link between oncogenic drivers and PD-L1 expression. Accordingly, Ebert *et al* (66) hypothesized that a dual blockade of MEK and PD-L1 might cause synergistic effects. Jiang *et al* concluded from their data that the potential therapeutic benefits of combining targeted inhibitors and immune modulation to improve patient outcomes should be investigated (67), a hypothesis which is supported by the results of the present study. Furthermore, the results from the EGFR blockade experiments point towards a similar direction, indicating that post-radiogenic activation of MAPK signaling most likely contributes to cellular defense in

response to treatment and can be tackled by EGFR inhibition in a context- and cell dependent manner.

The results of the present study are relevant as the efficacy of combined CRT and CPI is currently under investigation in clinical trials in HNSCC. However, expression patterns varied within the cell lines and exosomes examined. HNSCC are markedly heterogeneous. They include several subcategories related to anatomical location, etiology and molecular findings. The heterogeneity of HNSCC at the molecular level has hampered both the identification of specific targets and the development of targeted therapeutics for this entity. The results of the present study mirror the heterogeneity of HNSCC tumor cells and illustrate why the individualized characterization of checkpoint regulation is mandatory.

It is known that RT in combination with anti-PD-L1 agents stimulates CD8+ T cell-mediated anti-tumor immunity (68). If single dosages are applied, low dosages affect the vascularization of the tumor while higher doses are linked with innate and adaptive immune mechanisms via the mediation of type I interferon (IFN) (69). Hence, it is crucial to consider the sequence of application of treatment modules as well as the fractionation protocols which exert different effects on anti-tumor immune responses (70-72). In the current study and previously, the authors have assessed a combination scheme according to the clinically applied regimen for HNSCC patients to take the clonal selection of radioresistant tumor cells under fractionated irradiation into account (73).

The results of the present study are in part confirmed by results from other groups, yet, the current data situation is inconclusive. Fournel *et al* (74) have already described upregulation of PD-L1 by cisplatin in NSCLC. Park *et al* (75) stated that anti-PD-1 therapy may enhance several features of anti-tumor immunity that have been induced by platinum-based CT.

By contrast, Tran *et al* (76) demonstrated in a syngeneic oral cancer model that cisplatin could have immune-enhancing as well as immunosuppressive effects, which may be dose-dependent and partially reversible by combining PD-1/PD-L1 blockade. They discovered a robust increase in the $CD8^+$ T cell number of animals treated with anti-PD-1 alone which was not seen in animals treated with cisplatin and anti-PD-1. At present, it is unclear whether cisplatin can enhance or reduce anticancer immunity. However, this is an essential question as chemotherapy is frequently applied before or concurrent with CPI. One of the standard therapies in HNSCC is CRT, either in a definitive or an adjuvant approach. In this context, it seems important to assess a potential synergistic effect of this regimen on PD-L1 expression. In line with the results from Derer *et al* (68), the present study observed an upregulation at lower levels after single treatment with cisplatin compared with a combination exposure with fractionated RT.

Derer *et al* (51) suggested a tumor cell-mediated upregulation of PD-L1 expression following, in particular, CRT that is not only dependent on the somatic mutation prevalence of the tumor entity after discovering an upregulation of PD-L1 surface expression following fractionated irradiation in combination with dacarbazine. It is generally accepted that the prevalence of somatic mutations is associated with the immunogenicity of the tumor cells and tumors with a high mutational burden display a favorable response to immunotherapy.

The induction of PD-L1 by cisplatin has been validated by our previously established *ex vivo* 3D HNSCC model. The results support our observations *in vitro*. 3D validation is of importance to take tumor stroma interactions into account. Notably, similar effects of cisplatin on PD-L1 in HNSCC 2D and 3D cultures were found. These findings of the present study indicated that CRT has an effect on the increase of PD-L1 surface expression on tumor cells in the absence of immune cells. In this context, exosomes could serve as valuable biomarkers that reflect the therapeutic response and could be targeted directly to reduce exosome-mediated immunosuppression.

In general, establishing optimized and multimodal immunotherapy approaches could pave the way to a sensitivity towards CPI that is more robust and occurs in a greater proportion of patients. Combinations of ICI with anti-cancer and non-anticancer drugs are currently examined for beneficial effects in preclinical and early phase clinical trials (77-79).

Currently, the results of the present study are reviewed and validated in HNSCC 3D tumor models and it is strongly anticipated by preliminary data that the knowledge derived from the present study will be applicable to established cancers in patients exhibiting sensitivity to standard treatment. Designing and establishing novel multimodal schemes consisting of CRT with CPI will presumably help to overcome treatment resistance in HNSCC patients. Results from ongoing clinical trials in which CPI enter Standard of Care schemes are ardently awaited, however, as previously described, unselected patient collectives might not routinely experience benefits. For the guidance of novel drug combinations such as anti-TIM-3 (80) or vaccines along with (C)RT and CPIs, robust biomarker data from (pre-)clinical studies will be paramount.

In light of the data from the present study, taking a combined inhibition of the PD-1/PD-L1 axis and MAPK ERK signaling into account is suggested, which will be evaluated using 2D/3D HNSCC models in future studies. It is hypothesized that a complex context-dependent PD-L1 regulation exists in HNSCC undergoing chemoradio-/antibody therapy. Improved understanding of underlying mechanisms and overcoming the immunosuppressive effects of exosomes may provide the basis for the development of combinational therapies with higher efficacy and response rates for the treatment of HNSCC and other tumor types.

Acknowledgements

The authors gratefully acknowledge the excellent technical support of Ms. Petra Prohaska (Department of Otorhinolaryngology, Head and Neck Surgery, Medical Faculty Mannheim of the University of Heidelberg). They are indebted to Dr Stefan Hillmer (EMCF, University of Heidelberg) for assistance with the TEM micrographs and Dr Katja Nitschke (Department of Urology and Urosurgery, Medical Faculty Mannheim of the University of Heidelberg) for supporting the nanoparticle tracking analyses.

Funding

The work on 3D HNSCC models is substantially supported by the research funding program Development of Replacement

and Complementary Methods to Reduce Animal Testing provided by the Ministry of Rural Affairs, Food and Consumer Protection Baden-Wuerttemberg, Germany, to AA. (Staatshaushaltsplan 2020/2021 Kap. 0802, Tit. Gr. 74) and by the 3R network Baden-Wuerttemberg, Ministry of Science Baden-Wuerttemberg, Germany, to NR and KB. This research was funded by German Research Foundation (DFG) to SL (LU 2270/1-1).

Availability of data and materials

All data generated or analyzed during this study are included in this published article.

Authors' contributions

AA, KL, LT, MT, ES, AAz and SL were responsible for data curation. KL and LT were responsible for formal analysis. AA, NR and SL were responsible for funding acquisition. JS, MNT, AMR, JF, CAW, BK, AL and CS made substantial contributions to conception and design of the present study, the acquisition of data and analysis and interpretation of data. AA, JK, KB, NR and SL supervised the study. AA, LT, ES and SL were responsible for the diagrams. AA and SL wrote the original draft of the manuscript. AA, LT, MNT, JK, KB, NR and SL were responsible for writing, reviewing and editing the manuscript. AA and SL confirm the authenticity of all the raw data. All authors read and approved the final manuscript.

Ethics approval and consent to participate

Informed consent was obtained from all patients after review of the local ethics board (approval nos. 2019-528N, 2021-552 and 2019-697N).

Patient consent for publication

Not applicable.

Competing interests

The authors declare that they have no competing interests.

References

1. Sacco AG and Cohen EE: Current treatment options for recurrent or metastatic head and neck squamous cell carcinoma. J Clin Oncol 33: 3305-3313, 2015.
2. Burtness B, Harrington KJ, Greil R, Soulières D, Tahara M, de Castro G Jr, Psyrri A, Basté N, Neupane P, Bratland Å, *et al*: Pembrolizumab alone or with chemotherapy versus cetuximab with chemotherapy for recurrent or metastatic squamous cell carcinoma of the head and neck (KEYNOTE-048): A randomised, open-label, phase 3 study. Lancet 394: 1915-1928, 2019.
3. Gillison ML, Blumenschein G Jr, Fayette J, Guigay J, Colevas AD, Licitra L, Harrington KJ, Kasper S, Vokes EE, Even C, *et al*: CheckMate 141: 1-Year update and subgroup analysis of nivolumab as first-line therapy in patients with recurrent/metastatic head and neck cancer. Oncologist 23: 1079-1082, 2018.
4. Pardoll DM: The blockade of immune checkpoints in cancer immunotherapy. Nat Rev Cancer 12: 252-264, 2012.
5. Sun C, Mezzadra R and Schumacher TN: Regulation and function of the PD-L1 checkpoint. Immunity 48: 434-452, 2018.
6. Pai SI, Zandberg DP and Strome SE: The role of antagonists of the PD-1:PD-L1/PD-L2 axis in head and neck cancer treatment. Oral Oncol 61: 152-158, 2016.
7. Keck MK, Zuo Z, Khattri A, Stricker TP, Brown CD, Imanguli M, Rieke D, Endhardt K, Fang P, Brägelmann J, *et al*: Integrative analysis of head and neck cancer identifies two biologically distinct HPV and three non-HPV subtypes. Clin Cancer Res 21: 870-881, 2015.
8. Seiwert TY, Burtness B, Mehra R, Weiss J, Berger R, Eder JP, Heath K, McClanahan T, Lunceford J, Gause C, *et al*: Safety and clinical activity of pembrolizumab for treatment of recurrent or metastatic squamous cell carcinoma of the head and neck (KEYNOTE-012): An open-label, multicentre, phase 1b trial. Lancet Oncol 17: 956-965, 2016.
9. Chow LQM, Haddad R, Gupta S, Mahipal A, Mehra R, Tahara M, Berger R, Eder JP, Burtness B, Lee SH, *et al*: Antitumor activity of pembrolizumab in biomarker-unselected patients with recurrent and/or metastatic head and neck squamous cell carcinoma: Results from the phase Ib KEYNOTE-012 expansion cohort. J Clin Oncol 34: 3838-3845, 2016.
10. Soulieres D, Cohen E, Le Tourneau C, Dinis J, Licitra L, Ahn MJ, Soria A, Machiels JP, Mach N, Mehra R, *et al*: Abstract CT115: Updated survival results of the KEYNOTE-040 study of pembrolizumab vs standard-of-care chemotherapy for recurrent or metastatic head and neck squamous cell carcinoma. Cancer Res 78 (13 Suppl): CT115, 2018.
11. Ferris RL, Blumenschein G Jr, Fayette J, Guigay J, Colevas AD, Licitra L, Harrington K, Kasper S, Vokes EE, Even C, *et al*: Nivolumab for recurrent squamous-cell carcinoma of the head and neck. N Engl J Med 375: 1856-1867, 2016.
12. Gavrielatou N, Doumas S, Economopoulou P, Foukas PG and Psyrri A: Biomarkers for immunotherapy response in head and neck cancer. Cancer Treat Rev 84: 101977, 2020.
13. Ludwig S, Floros T, Theodoraki MN, Hong CS, Jackson EK, Lang S and Whiteside TL: Suppression of lymphocyte functions by plasma exosomes correlates with disease activity in patients with head and neck cancer. Clin Cancer Res 23: 4843-4854, 2017.
14. Cocucci E and Meldolesi J: Ectosomes and exosomes: Shedding the confusion between extracellular vesicles. Trends Cell Biol 25: 364-372, 2015.
15. van der Pol E, Böing AN, Harrison P, Sturk A and Nieuwland R: Classification, functions, and clinical relevance of extracellular vesicles. Pharmacol Rev 64: 676-705, 2012.
16. Ludwig S, Sharma P, Wise P, Sposto R, Hollingshead D, Lamb J, Lang S, Fabbri M and Whiteside TL: mRNA and miRNA profiles of exosomes from cultured tumor cells reveal biomarkers specific for HPV16-positive and HPV16-negative head and neck cancer. Int J Mol Sci 21: 8570, 2020.
17. Ludwig S, Marczak L, Sharma P, Abramowicz A, Gawin M, Widlak P, Whiteside TL and Pietrowska M: Proteomes of exosomes from HPV(+) or HPV(-) head and neck cancer cells: Differential enrichment in immunoregulatory proteins. Oncoimmunology 8: 1593808, 2019.
18. Theodoraki MN, Yerneni SS, Hoffmann TK, Gooding WE and Whiteside TL: Clinical significance of PD-L1^{+} exosomes in plasma of head and neck cancer patients. Clin Cancer Res 24: 896-905, 2018.
19. Theodoraki MN, Laban S, Jackson EK, Lotfi R, Schuler PJ, Brunner C, Hoffmann TK, Whiteside TL and Hofmann L: Changes in circulating exosome molecular profiles following surgery/(chemo)radiotherapy: Early detection of response in head and neck cancer patients. Br J Cancer 125: 1677-1686, 2021.
20. Jablonska J, Rist M, Spyra I, Tengler L, Domnich M, Kansy B, Giebel B, Thakur BK, Rotter N, Lang S and Ludwig S: Evaluation of immunoregulatory biomarkers on plasma small extracellular vesicles for disease progression and early therapeutic response in head and neck cancer. Cells 11: 902, 2022.
21. Daassi D, Mahoney KM and Freeman GJ: The importance of exosomal PDL1 in tumour immune evasion. Nat Rev Immunol 20: 209-215, 2020.
22. Gandara DR, Paul SM, Kowanetz M, Schleifman E, Zou W, Li Y, Rittmeyer A, Fehrenbacher L, Otto G, Malboeuf C, *et al*: Blood-based tumor mutational burden as a predictor of clinical benefit in non-small-cell lung cancer patients treated with atezolizumab. Nat Med 24: 1441-1448, 2018.
23. Rückert M, Flohr AS, Hecht M and Gaipl US: Radiotherapy and the immune system: More than just immune suppression. Stem Cells 39: 1155-1165, 2021.

24. Hecht M, Fietkau R and Gaipl US: Definitive chemoradiotherapy of locally advanced head and neck cancer in combination with immune checkpoint inhibition-new concepts required. Strahlenther Onkol 198: 83-85, 2022 (In German).
25. Welters MJ, Fichtinger-Schepman AM, Baan RA, Hermsen MA, van der Vijgh WJ, Cloos J and Braakhuis BJ: Relationship between the parameters cellular differentiation, doubling time and platinum accumulation and cisplatin sensitivity in a panel of head and neck cancer cell lines. Int J Cancer 71: 410-415, 1997.
26. Affolter A, Muller MF, Sommer K, Stenzinger A, Zaoui K, Lorenz K, Wolf T, Sharma S, Wolf J, Perner S, *et al*: Targeting irradiation-induced mitogen-activated protein kinase activation in vitro and in an ex vivo model for human head and neck cancer. Head Neck 38 (Suppl 1): E2049-E2061, 2016.
27. Hong CS, Funk S, Muller L, Boyiadzis M and Whiteside TL: Isolation of biologically active and morphologically intact exosomes from plasma of patients with cancer. J Extracell Vesicles 5: 29289, 2016.
28. Rajamoorthi A, Shrivastava S, Steele R, Nerurkar P, Gonzalez JG, Crawford S, Varvares M and Ray RB: Bitter melon reduces head and neck squamous cell carcinoma growth by targeting c-Met signaling. PLoS One 8: e78006, 2013.
29. Chu SC, Hsieh YS, Yu CC, Lai YY and Chen PN: Thymoquinone induces cell death in human squamous carcinoma cells via caspase activation-dependent apoptosis and LC3-II activation-dependent autophagy. PLoS One 9: e101579, 2014.
30. Chien MH, Yang WE, Yang YC, Ku CC, Lee WJ, Tsai MY, Lin CW and Yang SF: Dual targeting of the p38 MAPK-HO-1 axis and cIAP1/XIAP by demethoxycurcumin triggers caspase-mediated apoptotic cell death in oral squamous cell carcinoma cells. Cancers (Basel) 12: 703, 2020.
31. Chung EJ, Brown AP, Asano H, Mandler M, Burgan WE, Carter D, Camphausen K and Citrin D: In vitro and in vivo radiosensitization with AZD6244 (ARRY-142886), an inhibitor of mitogen-activated protein kinase/extracellular signal-regulated kinase 1/2 kinase. Clin Cancer Res 15: 3050-3057, 2009.
32. Leiker AJ, DeGraff W, Choudhuri R, Sowers AL, Thetford A, Cook JA, Van Waes C and Mitchell JB: Radiation enhancement of head and neck squamous cell carcinoma by the dual PI3K/mTOR inhibitor PF-05212384. Clin Cancer Res 21: 2792-2801, 2015.
33. Affolter A, Drigotas M, Fruth K, Schmidtmann I, Brochhausen C, Mann WJ and Brieger J: Increased radioresistance via G12S K-Ras by compensatory upregulation of MAPK and PI3K pathways in epithelial cancer. Head Neck 35: 220-228, 2013.
34. Affolter A, Fruth K, Brochhausen C, Schmidtmann I, Mann WJ and Brieger J: Activation of mitogen-activated protein kinase extracellular signal-related kinase in head and neck squamous cell carcinomas after irradiation as part of a rescue mechanism. Head Neck 33: 1448-1457, 2011.
35. Affolter A, Samosny G, Heimes AS, Schneider J, Weichert W, Stenzinger A, Sommer K, Jensen A, Mayer A, Brenner W, *et al*: Multikinase inhibitors sorafenib and sunitinib as radiosensitizers in head and neck cancer cell lines. Head Neck 39: 623-632, 2017.
36. Théry C, Witwer KW, Aikawa E, Alcaraz MJ, Anderson JD, Andriantsitohaina R, Antoniou A, Arab T, Archer F, Atkin-Smith GK, *et al*: Minimal information for studies of extracellular vesicles 2018 (MISEV2018): A position statement of the international society for extracellular vesicles and update of the MISEV2014 guidelines. J Extracell Vesicles 7: 1535750, 2018.
37. Ock CY, Kim S, Keam B, Kim S, Ahn YO, Chung EJ, Kim JH, Kim TM, Kwon SK, Jeon YK, *et al*: Changes in programmed death-ligand 1 expression during cisplatin treatment in patients with head and neck squamous cell carcinoma. Oncotarget 8: 97920-97927, 2017.
38. Barker HE, Paget JTE, Khan AA and Harrington KJ: The tumour microenvironment after radiotherapy: Mechanisms of resistance and recurrence. Nat Rev Cancer 15: 409-425, 2015.
39. Dovedi SJ, Adlard AL, Lipowska-Bhalla G, McKenna C, Jones S, Cheadle EJ, Stratford IJ, Poon E, Morrow M, Stewart R, *et al*: Acquired resistance to fractionated radiotherapy can be overcome by concurrent PD-L1 blockade. Cancer Res 74: 5458-5468, 2014.
40. Hirsch L, Zitvogel L, Eggermont A and Marabelle A: PD-Loma: A cancer entity with a shared sensitivity to the PD-1/PD-L1 pathway blockade. Br J Cancer 120: 3-5, 2019.
41. Kong Y, Ma Y, Zhao X, Pan J, Xu Z and Zhang L: Optimizing the treatment schedule of radiotherapy combined with anti-PD-1/PD-L1 immunotherapy in metastatic cancers. Front Oncol 11: 638873, 2021.
42. Narits J, Tamm H and Jaal J: PD-L1 induction in tumor tissue after hypofractionated thoracic radiotherapy for non-small cell lung cancer. Clin Transl Radiat Oncol 22: 83-87, 2020.
43. Kordbacheh T, Honeychurch J, Blackhall F, Faivre-Finn C and Illidge T: Radiotherapy and anti-PD-1/PD-L1 combinations in lung cancer: Building better translational research platforms. Ann Oncol 29: 301-310, 2018.
44. Wimmer S, Deloch L, Hader M, Derer A, Grottker F, Weissmann T, Hecht M, Gostian AO, Fietkau R, Frey B and Gaipl US: Hypofractionated radiotherapy upregulates several immune checkpoint molecules in head and neck squamous cell carcinoma cells independently of the HPV status while ICOS-L is upregulated only on HPV-positive cells. Int J Mol Sci 22: 9114, 2021.
45. Kikuchi M, Clump DA, Srivastava RM, Sun L, Zeng D, Diaz-Perez JA, Anderson CJ, Edwards WB and Ferris RL: Preclinical immunoPET/CT imaging using Zr-89-labeled anti-PD-L1 monoclonal antibody for assessing radiation-induced PD-L1 upregulation in head and neck cancer and melanoma. Oncoimmunology 6: e1329071, 2017.
46. Schulz D, Stancev I, Sorrentino A, Menevse AN, Beckhove P, Brockhoff G, Hautmann MG, Reichert TE, Bauer RJ and Ettl T: Increased PD-L1 expression in radioresistant HNSCC cell lines after irradiation affects cell proliferation due to inactivation of GSK-3beta. Oncotarget 10: 573-583, 2019.
47. Mutschelknaus L, Peters C, Winkler K, Yentrapalli R, Heider T, Atkinson MJ and Moertl S: Exosomes derived from squamous head and neck cancer promote cell survival after ionizing radiation. PLoS One 11: e0152213, 2016.
48. Taube JM, Klein A, Brahmer JR, Xu H, Pan X, Kim JH, Chen L, Pardoll DM, Topalian SL and Anders RA: Association of PD-1, PD-1 ligands, and other features of the tumor immune microenvironment with response to anti-PD-1 therapy. Clin Cancer Res 20: 5064-5074, 2014.
49. Snyder A, Makarov V, Merghoub T, Yuan J, Zaretsky JM, Desrichard A, Walsh LA, Postow MA, Wong P, Ho TS, *et al*: Genetic basis for clinical response to CTLA-4 blockade in melanoma. N Engl J Med 371: 2189-2199, 2014.
50. Ribas A and Hu-Lieskovan S: What does PD-L1 positive or negative mean? J Exp Med 213: 2835-2840, 2016.
51. Derer A, Spiljar M, Bäumler M, Hecht M, Fietkau R, Frey B and Gaipl US: Chemoradiation increases PD-L1 expression in certain melanoma and glioblastoma cells. Front Immunol 7: 610, 2016.
52. Oweida A, Lennon S, Calame D, Korpela S, Bhatia S, Sharma J, Graham C, Binder D, Serkova N, Raben D, *et al*: Ionizing radiation sensitizes tumors to PD-L1 immune checkpoint blockade in orthotopic murine head and neck squamous cell carcinoma. Oncoimmunology 6: e1356153, 2017.
53. Deng L, Liang H, Burnette B, Beckett M, Darga T, Weichselbaum RR and Fu YX: Irradiation and anti-PD-L1 treatment synergistically promote antitumor immunity in mice. J Clin Invest 124: 687-695, 2014.
54. Zhang B, Bowerman NA, Salama JK, Schmidt H, Spiotto MT, Schietinger A, Yu P, Fu YX, Weichselbaum RR, Rowley DA, *et al*: Induced sensitization of tumor stroma leads to eradication of established cancer by T cells. J Exp Med 204: 49-55, 2007.
55. Lin W, Chen M, Hong L, Zhao H and Chen Q: Crosstalk between PD-1/PD-L1 blockade and its combinatorial therapies in tumor immune microenvironment: A focus on HNSCC. Front Oncol 8: 532, 2018.
56. Rossi G, Russo A, Tagliamento M, Tuzi A, Nigro O, Vollome G Sini C, Grassi M, Bello MGD, Coco S, *et al*: Präzisionsmedizin bei NSCLC im zeitalter der immuntherapie: Neue biomarker zur selektion der am besten geeigneten therapie oder des am besten geeigneten patienten. Kompass Pneumol 8: 300-317, 2020.
57. Müller T, Braun M, Dietrich D, Aktekin S, Höft S, Kristiansen G, Göke F, Schröck A, Brägelmann J, Held SAE, *et al*: PD-L1: A novel prognostic biomarker in head and neck squamous cell carcinoma. Oncotarget 8: 52889-52900, 2017.
58. Balermpas P, Rödel F, Krause M, Linge A, Lohaus F, Baumann M, Tinhofer I, Budach V, Sak A, Stuschke M, *et al*: The PD-1/PD-L1 axis and human papilloma virus in patients with head and neck cancer after adjuvant chemoradiotherapy: A multicentre study of the German cancer consortium radiation oncology group (DKTK-ROG). Int J Cancer 141: 594-603, 2017.
59. Hong AM, Ferguson P, Dodds T, Jones D, Li M, Yang J and Scolyer RA: Significant association of PD-L1 expression with human papillomavirus positivity and its prognostic impact in oropharyngeal cancer. Oral Oncol 92: 33-39, 2019.

60. Chen G, Huang AC, Zhang W, Zhang G, Wu M, Xu W, Yu Z, Yang J, Wang B, Sun H, *et al*: Exosomal PD-L1 contributes to immunosuppression and is associated with anti-PD-1 response. Nature 560: 382-386, 2018.
61. Cordonnier M, Nardin C, Chanteloup G, Derangere V, Algros MP, Arnould L, Garrido C, Aubin F and Gobbo J: Tracking the evolution of circulating exosomal-PD-L1 to monitor melanoma patients. J Extracell Vesicles 9: 1710899, 2020.
62. da Silva JL, Dos Santos ALS, Nunes NCC, de Moraes Lino da Silva F, Ferreira CGM and de Melo AC: Cancer immunotherapy: The art of targeting the tumor immune microenvironment. Cancer Chemother Pharmacol 84: 227-240, 2019.
63. Theodoraki MN, Yerneni S, Gooding WE, Ohr J, Clump DA, Bauman JE, Ferris RL and Whiteside TL: Circulating exosomes measure responses to therapy in head and neck cancer patients treated with cetuximab, ipilimumab, and IMRT. Oncoimmunology 8: 1593805, 2019.
64. Ota K, Azuma K, Kawahara A, Hattori S, Iwama E, Tanizaki J, Harada T, Matsumoto K, Takayama K, Takamori S, *et al*: Induction of PD-L1 expression by the EML4-ALK oncoprotein and downstream signaling pathways in non-small cell lung cancer. Clin Cancer Res 21: 4014-4021, 2015.
65. Han JJ, Kim DW, Koh J, Keam B, Kim TM, Jeon YK, Lee SH, Chung DH and Heo DS: Change in PD-L1 expression after acquiring resistance to gefitinib in EGFR-mutant non-small-cell lung cancer. Clin Lung Cancer 17: 263-270.e2, 2016.
66. Ebert PJR, Cheung J, Yang Y, McNamara E, Hong R, Moskalenko M, Gould SE, Maecker H, Irving BA, Kim JM, *et al*: MAP kinase inhibition promotes T cell and anti-tumor activity in combination with PD-L1 checkpoint blockade. Immunity 44: 609-621, 2016.
67. Jiang X, Zhou J, Giobbie-Hurder A, Wargo J and Hodi FS: The activation of MAPK in melanoma cells resistant to BRAF inhibition promotes PD-L1 expression that is reversible by MEK and PI3K inhibition. Clin Cancer Res 19: 598-609, 2013.
68. Derer A, Frey B, Fietkau R and Gaipl US: Immune-modulating properties of ionizing radiation: Rationale for the treatment of cancer by combination radiotherapy and immune checkpoint inhibitors. Cancer Immunol Immunother 65: 779-786, 2016.
69. Burnette BC, Liang H, Lee Y, Chlewicki L, Khodarev NN, Weichselbaum RR, Fu YX and Auh SL: The efficacy of radiotherapy relies upon induction of type I interferon-dependent innate and adaptive immunity. Cancer Res 71: 2488-2496, 2011.
70. Lee Y, Auh SL, Wang Y, Burnette B, Wang Y, Meng Y, Beckett M, Sharma R, Chin R, Tu T, *et al*: Therapeutic effects of ablative radiation on local tumor require $CD8^+$ T cells: changing strategies for cancer treatment. Blood 114: 589-595, 2009.
71. Lugade AA, Moran JP, Gerber SA, Rose RC, Frelinger JG and Lord EM: Local radiation therapy of B16 melanoma tumors increases the generation of tumor antigen-specific effector cells that traffic to the tumor. J Immunol 174: 7516-7523, 2005.
72. Dewan MZ, Galloway AE, Kawashima N, Dewyngaert JK, Babb JS, Formenti SC and Demaria S: Fractionated but not single-dose radiotherapy induces an immune-mediated abscopal effect when combined with anti-CTLA-4 antibody. Clin Cancer Res 15: 5379-5388, 2009.
73. Rong C, Muller MF, Xiang F, Jensen A, Weichert W, Major G, Plinkert PK, Hess J and Affolter A: Adaptive ERK signalling activation in response to therapy and in silico prognostic evaluation of EGFR-MAPK in HNSCC. Br J Cancer 123: 288-297, 2020.
74. Fournel L, Wu Z, Stadler N, Damotte D, Lococo F, Boulle G, Ségal-Bendirdjian E, Bobbio A, Icard P, Trédaniel J, *et al*: Cisplatin increases PD-L1 expression and optimizes immune check-point blockade in non-small cell lung cancer. Cancer Lett 464: 5-14, 2019.
75. Park SJ, Ye W, Xiao R, Silvin C, Padget M, Hodge JW, Van Waes C and Schmitt NC: Cisplatin and oxaliplatin induce similar immunogenic changes in preclinical models of head and neck cancer. Oral Oncol 95: 127-135, 2019.
76. Tran L, Allen CT, Xiao R, Moore E, Davis R, Park SJ, Spielbauer K, Van Waes C and Schmitt NC: Cisplatin alters antitumor immunity and synergizes with PD-1/PD-L1 inhibition in head and neck squamous cell carcinoma. Cancer Immunol Res 5: 1141-1151, 2017.
77. Varayathu H, Sarathy V, Thomas BE, Mufti SS and Naik R: Combination strategies to augment immune check point inhibitors efficacy-implications for translational research. Front Oncol 11: 559161, 2021.
78. Califano JA, Khan Z, Noonan KA, Rudraraju L, Zhang Z, Wang H, Goodman S, Gourin CG, Ha PK, Fakhry C, *et al*: Tadalafil augments tumor specific immunity in patients with head and neck squamous cell carcinoma. Clin Cancer Res 21: 30-38, 2015.
79. Merlano MC, Merlotti AM, Licitra L, Denaro N, Fea E, Galizia D, Di Maio M, Fruttero C, Curcio P, Vecchio S, *et al*: Activation of immune responses in patients with relapsed-metastatic head and neck cancer (CONFRONT phase I-II trial): Multimodality immunotherapy with avelumab, short-course radiotherapy, and cyclophosphamide. Clin Transl Radiat Oncol 12: 47-52, 2018.
80. Kim JE, Patel MA, Mangraviti A, Kim ES, Theodros D, Velarde E, Liu A, Sankey EW, Tam A, Xu H, *et al*: Combination therapy with anti-PD-1, anti-TIM-3, and focal radiation results in regression of murine gliomas. Clin Cancer Res 23: 124-136, 2017.